PERGAMON

Chaos, Solitons and Fractals 11 (2000) 1855–1868

CHAOS
SOLITONS & FRACTALS

www.elsevier.nl/locate/chaos

The influence of stochastic behavior on the human threshold of hearing

Ilse Christine Gebeshuber [a,b,*]

[a] *TU-BioMed, University of Technology, Wiedner Hauptstr. 8-10/1145, A-1040 Vienna, Austria*
[b] *Physics Department, University of California, Santa Barbara, CA 93106, USA*

Abstract

The inner hair cells in the cochlea perform the crucial task of transforming mechanical sound signals into electrical activity. The cochlear nerve fibers code this information and convey it to the brain for further processing. This study investigates the performance of the system inner hair cell – primary auditory afferent nerve fibers at the physical limit of the mechano-electrical transduction for the human auditory frequency range. The Brownian motion of the hair cell's receptive organelle, the hair bundle, does not blunt the sensitivity, but in fact enlarges – especially in frequency regions which are most important for the perception of music and speech – via the mechanism of nonlinear stochastic resonance (SR) the dynamical range of the mechano-electrical transduction by at least one order of magnitude. The coding efficiency of small sinusoidal hair bundle deflections shows basic properties of the human hearing threshold curve for pure tones and corresponds to experimental results of noise-induced tuning curves in mechano-receptors in the rat foot. Furthermore, the model explains how altered coding efficiency contributes to pathological changes in the spiking pattern which arise from morphological changes in the hair bundle structure (e.g., in noise-induced sensorineural hearing loss of cochlear origin).

1. Introduction

In this study, the efficiency of the transduction of mechanical sound signals into the neural code (mechano-electrical transduction) is investigated for weak pure tones of several frequencies and intensities to get insight into the contribution of the inner hair cells and primary auditory afferents to the psychophysical human hearing threshold curve for pure tones (Fig. 1).

The hair cell, the internal ear's sensory receptor, is a mechanodetector of remarkable sensitivity. The hearing threshold occurs at a sinusoidal mechanical input that deflects the hair cell's receptive organelle, the hair bundle, by as little as ± 0.3 nm [3,45]. This motion of $\pm 0.003^{\circ}$ corresponds to a displacement of the pinnacle of the Eiffel Tower by only a thumb's breadth. For small displacements of a few nanometers, the hair cell's mechano-electrical sensitivity was estimated as about 0.2 mV/nm (turtle cochlear hair cell [3]) and 0.018–0.5 mV/nm (frog saccular hair cell [9]).

In the human inner ear, three rows of outer hair cells (OHCs) and one row of inner hair cells (IHCs) spiral up the cochlea. The task of OHCs is probably an enhancement of small signals, since they can generate forces capable of altering the delicate mechanics of the cochlear partition (see e.g. [37]), whereas IHCs mainly have afferent nerve fibers which conduct the coded information to the brain. Deflections of the hairs (stereocilia) of hair cells change the open probability of the transduction channels and result in receptor potential changes in the cells, which are a low-pass filtered image of stereociliary displacements, with

* Tel.: +43-1-58801-11461; fax: +43-1-58801-11499.
E-mail address: igebes@fbma.tuwien.ac.at (I.C. Gebeshuber).

0960-0779/00/$ - see front matter
PII: S0960-0779(99)00122-8

additional stochastic components due to endogenous noise. The relationship between cochlear place and the regions of greatest frequency sensitivity in man is given by the equation $f = 200(10^{2d} - 0.7)$ [19], where d is the normalized distance along the cochlea measured from the apex and f is the characteristic frequency of the nerve fiber.

In so-called active zones at the base of the hair cell, sufficient depolarization of the receptor potential evokes Ca^{2+}-induced release of vesicles filled with neurotransmitter. This causes the generation of action potentials in cochlear nerve fibers. Stimulation at threshold evokes a receptor potential of $\approx$100 μV [3], which evidently suffices for reliable synaptic transmission.

Not even thermal motion of the hair bundle limits the sensitivity of the cell, i.e., its responsiveness, as the experimental results of Denk and co-workers demonstrate for saccular hair cells of the frog [6,7,10]. They showed that the mechanical properties of sensory hair bundles are reflected in their Brownian motion. A focused, low-power laser beam was used to measure the spontaneous deflection fluctuations of the sensory hair bundles on frog saccular hair cells with a sensitivity of about 1 $\mathrm{pm}/\sqrt{\mathrm{Hz}}$. The r.m.s. displacement of approximately 3.5 nm at a hair bundle's tip suggested a stiffness of about 350 μN/m, a result, which is in agreement with measurements made with a probe attached to a bundle's tip. The spectra, measured over a range of frequencies from 1 Hz to 20 kHz, resemble those of overdamped harmonic oscillators with roll-off frequencies between 200 and 800 Hz. The hair bundle motion is mainly damped by the surrounding fluid because the roll-off frequencies depend strongly on the viscosity of the bathing medium.

The forward and reverse transduction at the limit of sensitivity was studied by Denk and Webb [9] by correlating electrical and mechanical fluctuations in frog saccular hair cells. The spontaneous fluctuations of the intracellular voltage and the position of the sensory hair bundle were measured concurrently using intracellular microelectrodes and an optical laser differential micro interferometer [8]. Magnitude and frequency distributions of the hair bundles' spontaneous motion suggest that it consists mainly of Brownian motion. The electrical noise of the receptor potential exceeds the value expected for thermal Johnson noise, and its frequency distribution reflects the transduction tuning properties of the hair cells. Frequently, a strong correlation was observed between the fluctuations of the hair bundle position and the intracellular electrical noise.

From the properties of the correlation and from experiments involving mechanical stimulation it can be concluded that in most cases mechano-electrical transduction of the bundles' Brownian motion caused this correlation. Small signal transduction sensitivities ranged from 0.018 to 0.5 mV/nm. Bundle motion that was observed in response to current injection in more than half of the cells suggested the existence of a fast reverse (electro-mechanical) transduction mechanism to be common in these cells. The sensitivities could be as high as 600 pm of bundle deflection per mV of membrane potential change.

Hudspeth et al. [24] measured the forces that are necessary to open a single transduction channel in a hair cell to be 290 fN. They assumed that a displacement of the hairs of the hair cell of about 4 nm is enough to open the first transduction channel. However, since the transduction channels are continually opening and closing under the influence of thermal energy (thermal switching), and since deflection at threshold levels merely causes a redistribution of the open and closed states, the actual definition of threshold becomes a statistical one, and dependent on the amount of average employed.

Because a single fiber cannot respond over the full hearing range of 120 dB, intensity must be coded in a population of fibers with different thresholds. Highly spontaneous cochlear fibers with very low threshold are up to 80 dB more sensitive than cochlear fibers with no spontaneous discharge and very high thresholds of similar characteristic frequency [31]. About two-thirds of the afferent cochlear nerve fibers are highly sensitive, i.e., they have a high spontaneous rate. Spontaneous activity in single nerve fibers was measured to be up to 140 spikes/s and is present in the absence of any acoustic stimulation [41]. Note that this spontaneous spiking does not lead to any sensory perception, which reflects the ability of the brain to suppress noise.

Modeling studies show that the transduction mechanism is so sensitive that voltage fluctuations arising because of the Brownian motion of the hair bundle, which is free standing in the inner hair cells of the mammalian cochlea, and other endogenous noise sources in the hair cell, like noise due to thermal switching of the transduction channels and Johnson noise contribute to the spontaneous activities of auditory nerve fibers [48].

It has long been known that the auditory system preserves temporal information. Listeners use temporal cues, along with others, in encoding the low-frequency information in our language (the vowel sounds) and

in preserving smallest interaural time differences used in localizing the source of a sound in space (for a comprehensive survey of spatial hearing, see [1]). Temporal coding comes about because the hair cells in the cochlea are functionally polarized, which means that deflection of the stereocilia in one direction is excitatory and movement in the opposite direction is inhibitory. Thus, when the basilar membrane vibrates in response to low- and mid-frequency signals, below about 4 kHz, the hair cells in the region of vibration exhibit an alternating excitation-inhibition at the frequency of vibration. This, in turn, generates action potentials in auditory nerve fibers attached to those hair cells. The action potentials in the nerve reflect the time pattern of excitation and inhibition in the hair cell. The result is a train of nerve impulses time locked to the individual cycles of the acoustic stimulus. For a simple sine wave, the impulses are generated around a particular point on the sine-wave cycle, a process that is referred to as phase-locking. Because of its refractory period, which is about 0.8 ms in cat [27], an auditory nerve fiber cannot respond to every successive cycle of a stimulus. When it responds, however, it does so around a constant phase angle of the stimulus. Consequently, the impulses occur around integral multiples of the period of the sinusoidal stimulus.

The first neural responses at barely threshold intensities appear to be a decrease in spontaneous activity, and phase-locking of spike discharges to the stimulus cycle. Though the overall discharge rate may not be significantly greater than the spontaneous level, those spikes that do occur will tend to be locked in phase with the stimulus cycle [22,43,44] and therefore give information about the stimulus frequency. This may occur at an intensity far below the one which results in an increase of the mean firing rate: e.g. [18] report phase-locking on average 9 dB (= a factor of 2.8) below discharge rate threshold.

When the stimuli get stronger, the spiking rate increases. An astounding sensitivity of this rate modulation was measured in 1984 by Narins and Lewis [36] in the neotropical frog *Leptodactylus albilabris*, which exhibits the greatest sensitivity to substrate-borne vibrations (seismic stimuli) reported to date for any terrestrial animal: the vibration of the entire frog by one-tenth of an Ångström produces a modulation of about 10 spikes per second in neurons from the sacculus, an organ of hearing in fish and of balance in man. Furthermore, they report that single vibration-sensitive fibers in the white-lipped frog saturate at whole animal displacements of 10 Å peak to peak. Assuming a conservative 20 dB dynamic range for these fibers, the in vivo frog sacculus and the mammalian cochlea exhibit roughly equal sensitivities to displacement.

2. Materials and methods

The overall stereociliary displacement is the sum of the weak stimulus and the displacements due to Brownian motion. Stereociliary displacements change the open probability of the transduction channels, and evoke receptor potential changes, which add to fluctuations arising due to Johnson noise and other endogenous noise sources in the hair cell, namely the thermal switching of the ion channels (transduction channels, basolateral channels). The analysis of interspike interval histograms of spike trains which are elicited in cochlear afferents conveys information about the coding efficiency of signals with several frequencies and intensities.

2.1. Endogenous noise sources in the system

Endogenous noise sources in the hair cell are the Johnson noise due to thermal agitation of charge in conductors, the thermal noise due to ion channel switching in the membrane, the voltage noise which is induced via the thermal motions of the stereocilia and the variability of neurotransmitter release. Noise sources in the afferent nerve fibers arise because of thermal switching of ion channels in the excitable membrane.

2.1.1. Johnson noise in the IHC

Johnson noise (also called Nyquist noise, since the theoretical basis of Johnson noise is the Nyquist theorem), i.e., electrical fluctuations due to thermal agitation of charge in conductors, is independent of the

material and the shape of the conductor. At room temperature, the constancy of voltage noise variance per unit resistor bandwidth both for electronic and ionic conductors is (expressed in terms of power)

$$\frac{(V^2)_m}{R} \cong 10^{-18}\ \mathrm{W}$$

for any conductor.

$(V^2)_m$, the squared r.m.s. transmembrane thermal Johnson noise voltage for a parallel RC circuit, is given by

$$(V^2)_m = 2kTR \int_{-\infty}^{\infty} \frac{1}{1 + (2\pi fRC)^2}\ \mathrm{d}f = \frac{kT}{C}.$$

$(V^2)_m$ is finite because higher frequencies from the noise source in R are shortened to ground through C. $(V^2)_m$ does not depend on R: as R becomes larger, the noise source ($4kRT$) increases, but the roll-off frequency $1/(2\pi RC)$ decreases and the two effects cancel [5].

Since the IHC membrane capacitance is about 9.6 pF [29], the IHC r.m.s. transmembrane thermal Johnson noise voltage is about $\sqrt{(V^2)_m} = 21.2$ μV at body temperature. In our model for the IHC [39] the membrane capacitance is 11.058 pF, and therefore, $\sqrt{(V^2)_m} = 19.7$ μV at body temperature (310 K).

2.1.2. Endogenous IHC transduction channel noise

The open probability of the transduction channels for undeflected stereocilia is about 15% [23,35,49]. There are few data available on the kinetics of transduction channels. Crawford et al. [4] report for a 150 nm displacement of turtle hair cell stereocilia a mean open time of 1.1 ms and a distribution that could be well fitted by a single exponential. Because of this, the open/close kinetics are modeled by a Markovian process without memory (i.e., at any instant of time, the open probability is just dependent on stereociliary deflection, and not on the time the channel already has been open or closed). The shortest possible transduction channel open time is assumed to be 0.01 ms, the closed time histogram shows the typical exponential decay which is known from experiments [17,46].

2.1.3. Noise of the IHC basolateral channels

According to our model of the IHC [39] the K^+ channels in the lateral cell body membrane are modeled as being always open. Therefore they do not contribute to any noise in the IHC model. This is an unrealistic situation, firstly, because of course the K^+ channels show thermal switching, as well as voltage dependent changes in their kinetics, and secondly, there are other channels in the basolateral cell body membrane. This modeling assumption is only justified since too few data on the kind of the respective channels as well as on their number and on their kinetics are available, especially for human or more generally mammalian IHCs.

2.1.4. Deflection noise due to IHC stereociliary Brownian motion

The Brownian motion of the tips of the stereocilia is calculated using a reduced version of the stereocilia linear chain model of Svrcek-Seiler et al. [48]. The overall displacement x of the hair bundle for stimulation with weak signals is the sum of the bundle displacements due to Brownian motion x_{Brown} and the deterministic signal induced displacements x_{det}:

$$x = x_{\mathrm{Brown}} + x_{\mathrm{det}}.$$

x_{Brown} is calculated by integrating the velocity of the stereociliary bundle in the physiologically relevant x direction. Displacements toward $+x$ result in an increased open probability of the transduction channel, displacements toward $-x$ result in an decreased open probability. In the resting state, about 15% of the 60 transduction channels in the model human IHC are open.

$$x_{\mathrm{Brown}} = \int v_x\ \mathrm{d}t.$$

The stereociliary bundle velocity v_x in the physiologically relevant direction at time t is (for parameters see Table 1)

Table 1
Parameters (from Denk et al. [10]) used for modeling the reduced version of the stereocilia linear chain model

Parameter	Value
Undamped angular eigenfrequency (the stiffness C of a stereocilium is the ratio between an external horizontal force applied to its tip and the resulting horizontal tip displacement)	$\omega_0 = \sqrt{3C/m} = \sqrt{3.5 \times 10^{10} s^{-2}}$
Damping constant	$\beta = 1.27 \times 10^7$ s^{-1}
Integration step size	cint $= 10^{-6}$ s
Correlation time constant of the noise, giving a break frequency of $1/(2\pi\tau)$ Hz	$\tau = 10^{-15}$ s (should be at least twice the size of the integration interval)
Standard deviation of the Ohrnstein–Uhlenbeck noise	sig $= 3.297 \times 10^{-3}$ m/s^2
Mass	$m = 1 \times 10 \cdot 10^{-14}$ kg

$$v_{x,t} = \int \left(-\omega_0^2 \cdot x_{\text{Brown}} - \beta \cdot v_{x,t-1} + \frac{\text{rnd}}{\text{cint}} \right) \text{d}t.$$

The random number rnd is modeled as an Ohrnstein–Uhlenbeck noise (zero mean, standard deviation depending on temperature T, mass m, damping constant β in physiological conditions) and the integration step size cint:

$$\text{rnd} = \text{ou}(\tau, 0, \text{sig}),$$

$$\text{sig} = \sqrt{\frac{2kT}{m} \cdot \beta \cdot \text{cint}}.$$

The r.m.s. value of the modeled intrinsic bundle noise, x_{Brown}, is 2.12 nm, which is in accordance with experimental data [10]. In vestibular hair cells of the frog, vicious drag acting on the bundle limits Brownian motion to relatively low frequencies (200–800 Hz [10]). However, our theoretical considerations suggest for thermal fluctuations in mammalian hair cells a corner frequency of some kHz [48], which means that stochastic resonance is also effective in the mid-frequency range of audition.

The small amplitude of the fluctuations due to Brownian motion can be appreciated by comparing them to the dimensions of a single stereocilium, which is about 0.2 μm in diameter, or to the bundle's displacement–response relationship (Fig. 2).

x_{det} is a sinusoidal stimulus with a given amplitude amp and a given angular frequency ω:

$$x_{\text{det}} = \text{amp} \cdot \sin(\omega \cdot t).$$

2.1.5. Voltage noise in the IHC

The endogenous noise sources described above cause spontaneous receptor potential fluctuations in the unstimulated IHC: for small displacements to the lateral side ($+x$) the transduction channel open probability increases and herewith the influx of potassium ions which cause a depolarization of the receptor potential from its resting state, which is about −40 mV for IHCs (see e.g. [2]). Respectively, displacement to the medial side ($-x$) decreases the open probability, less potassium ions enter the cell and the potential hyperpolarises (Fig. 2).

The receptor potential fluctuations in the IHC are calculated via the reduced model for the mechano-electrical transduction in IHCs [40]. For displacements in the range of a few nm, the relation between stereociliary displacement and open probability of the transduction channels is linear (Fig. 2). Since the IHC membrane time constant is $\tau = 0.255$ ms [39], the IHC potential is a low-pass filtered figure of the stereociliary displacements with additional noise because of the stochastic components described above (Fig. 3).

2.1.6. Jitter in the spiking times of the cochlear nerve fibers

Since the system has internal noise sources which mix with the input signal, precise relations between the temporal features of the signal at the input and the output spikes will be randomized to a certain degree.

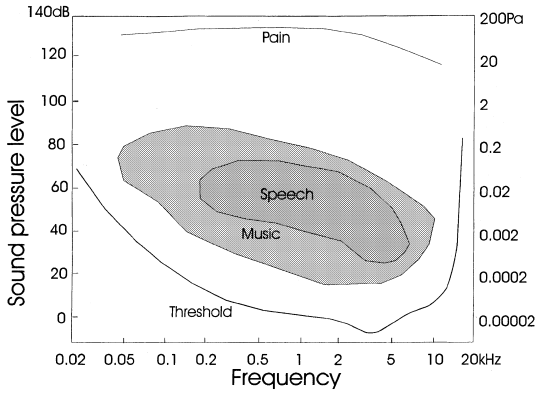

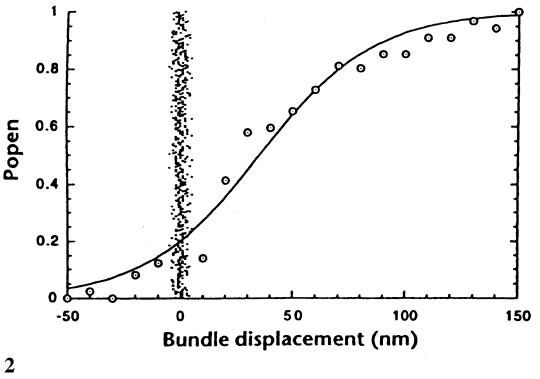

Fig. 1. Psychophysically measured hearing area, i.e., the range between hearing threshold and pain threshold. The intensity is scaled in dB, the pressure is scaled in Pa. Note that the intensity covers 14 orders of magnitude. Adapted from Zwicker [50].

Fig. 2. The relation of a 250 ms time trace of simulated Brownian motion (low-pass filtered, 2 nm r.m.s. white noise applied to a hair bundle) to a cell's displacement–response relationship, which relates the open probability of transduction channels to the hair bundle displacement. Note that in this specific case the transduction channel resting open probability is 0.2. From Jaramillo and Wiesenfeld [26].

This means the fiber may respond differently each time a stimulus of a certain strength is applied to the hair cell, since fluctuations in excitability and latency are directly associated with fluctuations in the resting membrane potential [11].

Endogenous noise in the resting neural membrane potential of nerve fibers decreases with increasing diameter, e.g. it is in the order of 1 mV r.m.s. for myelinated fibers with small diameter, and less than 1 mV for myelinated fibers with larger diameter [12]. In man, the auditory nerve comprises about 30,000 fibers, all myelinated [21]. The mean inner diameter of the central axons of these fibers has an unimodal distribution and ranges between 2.7 and 3.1 μm, with the exception of more smaller fibers at the lower (i.e., high-frequency) cochlear end [47]. Lass and Abeles [30] showed that propagation of the action potential is relatively noise free, with a 10 cm length of myelinated axon introducing only a few microseconds of jitter in the arriving time of a spike. What remains as significant noise source is synaptic transmission [28].

The spike generating process is simulated as follows: any time the voltage fluctuations in the IHC exceed the threshold of 0.1 mV, a value which is sufficient for neurotransmitter release in hair cells [3,23], a spike can be generated in the afferent nerve fibers connecting to the hair cell. Since not every time the voltage exceeds the threshold of 0.1 mV a spike is produced, the probability for spiking is adjusted to a mean spontaneous spiking rate of about 100 Hz [41]. Jitter in the firing times is modeled with positive values of a normally distributed time shift with zero mean and a standard deviation of 50 μs. Since the absolute refractory period, i.e., the minimum time between two spikes in a single nerve fiber, is about 0.8 ms in cat [27], the time constant of the exponentially decaying threshold curve is set to 0.25 ms, the maximum value for the height is 2 mV (Fig. 4).

2.2. Temporal coding of frequency information in interspike interval histograms

The efficiency of temporal coding is investigated by analysis of the interspike interval histograms (ISIHs), bar charts representing the interspike interval distribution. The heights of the bars represent the number of occurrences of a certain range of interspike times. This range of interspike times is determined by the binwidth.

ISIHs are calculated for several frequencies within the human audible frequency range and for various small signal-to-noise ratios (snr). Snr is defined as the relation between the r.m.s. of the signal and the r.m.s. of the stereociliary deflections due to Brownian motion. Increasing snr is characterized by an increase in the amplitude of the stereociliary deflection, the noise being the endogenous noise in the hair cell. When there is no signal present (snr = 0), the distribution in the histogram is Poisson-like. With increasing snr, the spikes

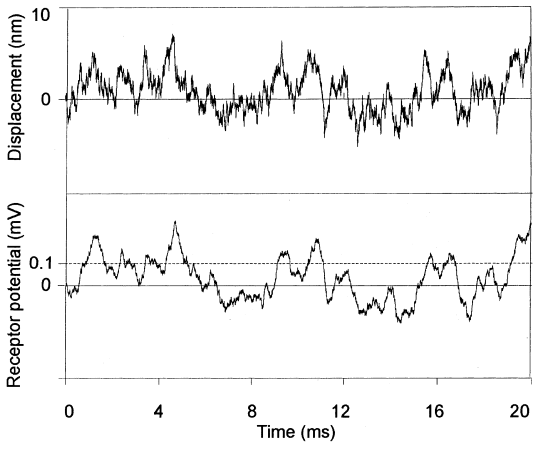

3

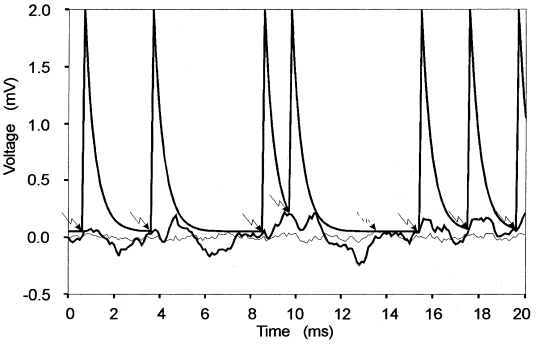

4

Fig. 3. Modeled inner hair cell mechanical and electrical fluctuations due to Brownian motion: the intracellular receptor potential changes (bottom trace) are a low-pass filtered figure of stereociliary displacements (top trace) with an additional portion of noise resulting from transduction channel kinetics.

Fig. 4. Simulated receptor potential changes and resulting firing behavior. The noise in the voltage fluctuations evoked by a weak 500 Hz signal alone (thin line, hypothetical case without Brownian motion) is a consequence of the endogenous transduction channel noise. Only in one case (marked by dashed arrow at 13.5 ms) those fluctuations are large enough to reach the threshold for spiking at 0.1 mV. The compound fluctuations caused by the sinusoidal tone and the thermal fluctuations with a snr of 0.2 show the enhancing effect of the noise: Seven spikes occur within 20 ms, they are distributed to connecting auditory nerve fibers. The recovery behavior after spiking is modeled by an exponential decay of the threshold curve: as soon as the voltage fluctuations again cross the threshold curve, a new spike can occur.

tend to be more phase-locked. When the binwidth of the histograms is chosen half the period duration of the stimulating signal, phase-locking of the interspike times can be seen in the ISIH as an up–down–up–down pattern: more spikes appear at interspike times which are odd multiples of the half of the period duration of the sinusoidal stimulus. The maximum interspike time considered is 20 ms, according to Rose et al. [44]. The histograms contain data from one second stimulus duration. Since the Brownian motion of the stereocilia is an ergodic process and the noise sources to independent fibers are assumed to be independent, this time is equivalent to shorter stimulus durations, if one considers spikes of fibers coming from adjacent hair cells which are stimulated by the traveling wave.

Because of stochastic behavior in the spike generation process, a higher number of spikes included in the ISIH increases the information content and its reliability. The innervation density is a nonlinear function of frequency (i.e., of the position of the IHCs in the tonotopically organized cochlea), decreases at the high- and low-frequency ends of the cochlea and reaches its maximum of about 15 nerve fibers per IHC in the mid-frequency region which is most important for speech and music (Table 2; [15,47]). Therefore, for a given stimulus duration, the number of available spikes per IHC and unit time is dependent on tonotopic location.

3. Results

We investigate the efficiency of coding by analysis of ISIHs of the spike trains elicited in cochlear nerve fibers connecting to single hair cells. The stimuli are weak sinusoidal stereociliary deflections with snr from 0 to 1, which equals displacements of the stereocilia with amplitudes between 0 and 2.12 nm r.m.s., since the 2.12 nm r.m.s. stereociliary displacement noise is taken as reference for calculation of the snr. The frequencies of the stimulating deterministic signals range between 200 and 20 kHz.

Fig. 5 shows ISIHs of spike trains resulting from 200 Hz deterministic stereociliary displacements. With increasing snr, the ISIH changes its shape, the longer interspike times tend to disappear, and the up–down structure becomes clearly visible.

Table 2
The binwidth is chosen in half the period duration of the stimulus, to visualize the phase-locking effect as an up–down structure in the interspike interval histograms. The maximum interspike time is fixed to 20 ms, therefore the number of bins per histogram increases with frequency. The right column gives the number of highly sensitive cochlear afferents for inner hair cells from the respective tonotopic locations along the cochlea (human data from Spoendlin and Schrott [47] and Felix et al. [15])

Frequency (Hz)	Binwidth (ms)	# of bins	# of nerve fibers
100	5	4	3
200	2.5	8	5
500	1	20	9
1000	0.5	40	12
2000	0.25	80	9
5000	0.1	200	8
10,000	0.05	400	6
20,000	0.025	800	3

Fig. 6 (note that the maximum interspike time shown is 10 ms) and the left trace of Fig. 7 show the effect of changing the binwidth. Both histograms are based on the same data set, but in Fig. 6 the binwidth is 0.05 ms, 1/10 of the binwidth in Fig. 7. The interspike times have multimodal normal distributions. This information is lost in the case with the larger binwidth. For stimulation with 1 kHz, the spikes tend with increasing snr to occur more and more in the first halves of multiples of the period duration, i.e., the phase-locking effect becomes more and more visible (Fig. 7).

The phase-locking effect is clearly lost for frequencies above 5kHz, since the influence of jitter, which causes a delay in the spiking time, gets larger with increasing frequency.

With decreasing frequency, the number of bins and therefore the possibility of any fine structure information decreases in the ISHI.

A means to assess the information which is contained in the ISIH is the relation between the spikes which occur during the positive half-wave of the stimulating signal and the total number of spikes. This gives the percentage of informative spikes.

In this way, for every investigated signal frequency and snr, one number was obtained: the percentage of informative spikes. The frequency–response efficiency tuning curves for several snr as presented in Fig. 8 give the percentage of informative spikes for various frequencies and snr. The curves for small snr may be called human hearing threshold curves for pure tones as they are caused by the effects of stereociliary Brownian motion, endogenous hair cell noise, stochasticity in neurotransmitter release and innervation density of primary auditory afferents in various frequency bands. But note that this modeling study presents threshold curves as they are imposed by the transduction of small sinusoidal displacements of the stereocilia, which arise at the IHC after the chain of outer ear, middle ear, basilar membrane, cochlear duct, and amplification by OHCs. Furthermore, any possible effect of the inhibitory efferent innervation of the IHC afferent nerve fibers (see e.g. [13,14]) on the spiking pattern is neglected because of a lack of experimental data.

The curves are V-shaped, with 1 kHz as best frequency. Above 5 kHz the phase-locking effect completely disappears, therefore for 10 and 20 kHz only the $\mathrm{snr} = 1$ case was simulated.

At 200 Hz, increasing the snr also increases the number of informative spikes: at a snr of 0.1, the number of informative spikes is 40% (mainly caused by the large period duration of 5 ms, therefore a histogram binwidth of 2.5 ms), and with increasing snr, the number of informative spikes slowly increases up to 66%. Although the number of informative spikes is still larger than 50% for the 200 Hz signal in the $\mathrm{snr} = 0.2$ case (Fig. 5), the number of events in each bin tends to decrease exponentially with increasing interspike time (similar to the $\mathrm{snr} = 0$ case). The fine structure with valleys for multiples of the negative half-wave of the stimulating signal is for a weak 200 Hz stimulus only for a snr of 0.5 or more present. For some of the histograms for the 200 Hz signal see Fig. 5.

At 500 Hz and snr above zero, the number of informative spikes is always above chance (i.e., above 50%). Of course, 52.6% informative spikes, as is the case for $\mathrm{snr} = 0.1$, means only about two more phase-locked spikes per nerve fiber and second, but by getting this information in the spikes' trains arriving in parallel from many IHC might be enough to enable the brain extract this information from the statistics (for an "Homage to the single spike", see [42, p. 279]).

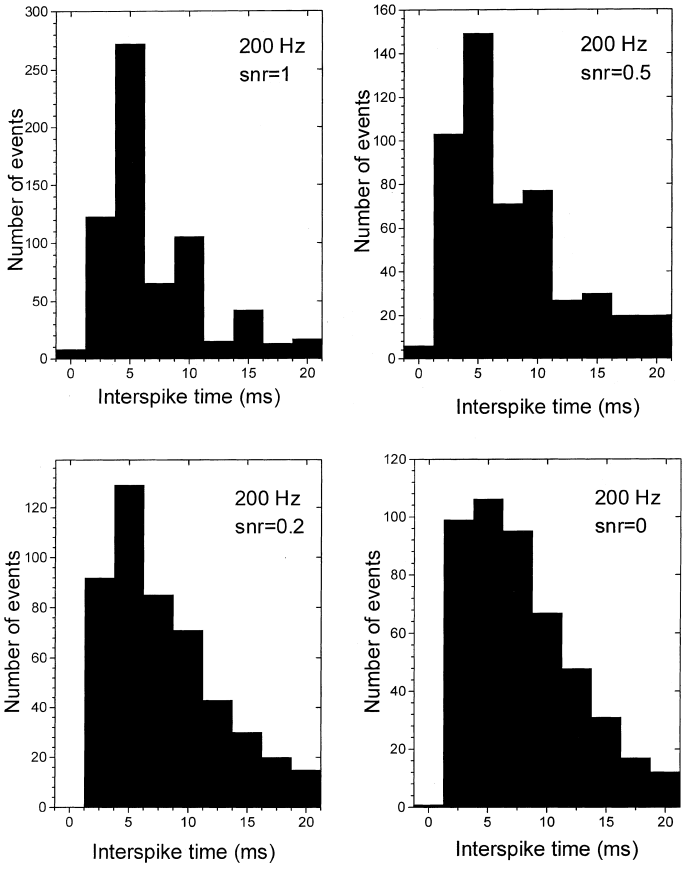

5

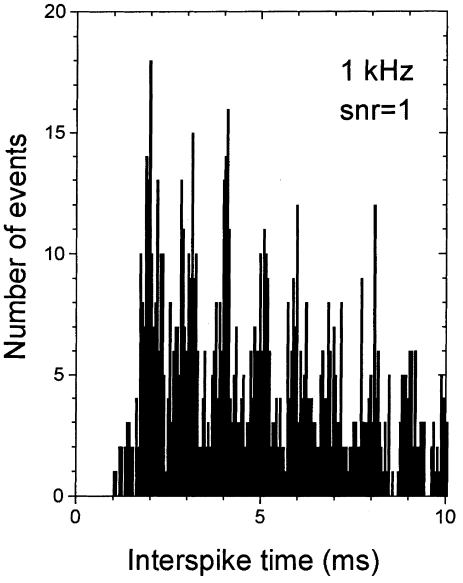

6

Fig. 5. Interspike interval histograms (ISIHs) for a 200 Hz signal with a snr of 0, 0.2, 0.5 and 1. Stimulus duration 1 s, 5 highly sensitive nerve fibers, binwidth 2.5 ms.

Fig. 6. ISIH for a 1 kHz signal with a signal-to-noise ratio of 1. Stimulus duration 1 s, binwidth 0.05 ms, 12 highly sensitive nerve fibers. The phase-locking effect is clearly visible. Same data set as for Fig. 7, but note that only interspike times up to 10 ms are shown.

At 1 kHz, the frequency which can be coded and decoded best under the given circumstances, a reversal of the shape of the curve appears for very small snr. When the signal gets stronger, the curve inverts and gets sharper. This effect corresponds to experimental results in noise-induced tuning curve changes in mechanoreceptors of the rat foot [25]. In this paper, Ivey and coworkers give a theoretical explanation for the reversal of the shape, whose analogue for the modeled frequency-response efficiency tuning curves in the IHC is the following: our model of the transduction process results in frequency-dependent receptor potentials. For low and high frequencies, the subthreshold deterministic stimuli elicit voltage changes further from the threshold than the ones elicited by mid-frequency stimuli. Therefore, the optimal noise level is also frequency dependent, and the inversion of the tuning-curve for stimuli with small snr is directly related to the threshold shift (see Fig. 8 from [25]).

The 2 kHz case is qualitatively comparable to the 1 kHz case. Increasing snr increases the number of informative spikes, from about (but higher than) chance in the $\mathrm{snr} = 0.1$ case to over 70% in the $\mathrm{snr} = 1$ case.

At 5 kHz the jitter destroys most of the phase-locked information in the cochlear afferents. However, statistics over a longer period would still resolve some information, at least for snr close to one and higher.

In the 10–20 kHz regime, increasing the signal does not increase the number of informative spikes, since the jitter completely destroys the phase-locking information. Therefore, the psychophysical hearing threshold data for this high-frequency regime cannot be explained by phase-locking. This means that in the

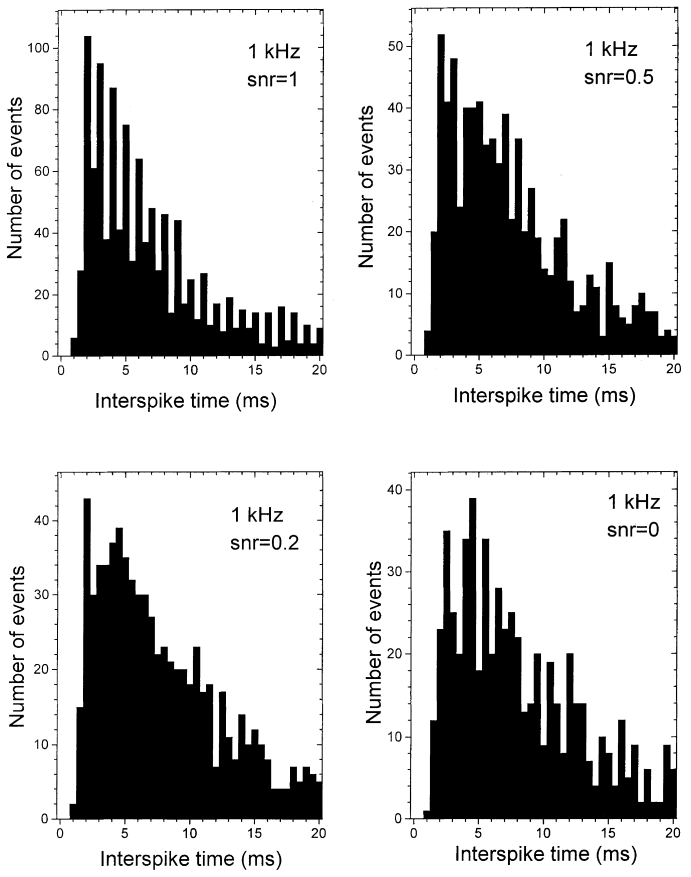

Fig. 7. ISIHs for a 1 kHz signal with several snrs. With increasing snr, the number of spikes in multiples of the first halves of the period duration (informative spikes), increases. Stimulus duration 1 s, 12 highly sensitive nerve fibers, binwidth 0.5 ms.

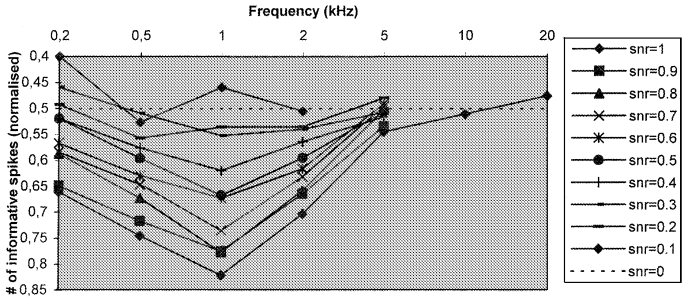

Fig. 8. Frequency-response efficiency tuning curves for the multicellular model for peripheral auditory coding, i.e., normalized number of informative spikes for several frequencies and snrs. For snr = 0 there is no signal present, and half of the spikes are phase-locked because of chance (i.e., the normalized number of informative spikes is 0.5). For frequencies between 0.2 and 2 kHz, the phase-locking effect increases with increasing snr, i.e., the normalized number of informative spikes increases well above 0.5. In the 5 kHz case there is nearly any phase-locking effect visible (therefore the snr = 0.1 case was not modeled). The 10 and 20 kHz cases show no effect of phase-locking at all. Therefore in these cases only the normalized number of informative spikes for snr = 1 are presented. For high snr (strong signal) the curves are *V*-shaped, when the signal gets weaker and the influence of noise increases, the curves broaden and eventually invert at 1 kHz. Stimulus duration for each data point 1 s. For frequency-dependent innervation density see Table 2.

high-frequency regions, frequency information must be coded in a different way. The increase in spiking rate from many cochlear afferents of neighbored hair cells is the proper candidate for supplying this information.

4. Discussion

In this multicellular model for peripheral auditory coding the enhancing effect of Brownian noise on the high sensitivity of the auditory system was demonstrated (Fig. 4). It was shown that the noise quantitatively accounts for the detection of weak pure tones which would otherwise either evoke receptor potentials too small to elicit spikes at all or too few spikes sufficient for determination of the stimulus frequency.

The ISIHs are calculated for a single IHC with frequency dependent innervation density and a stimulus duration of one second. The more highly sensitive afferents are connected to one IHC, the more data are available for the ISIH. Therefore, increasing innervation density increases the reliability of the information obtained from analysis of the histograms.

In reality, the brain does not only get the information about the signal from just one hair cell, but from many (the higher the intensity, the more hair cells respond, since a larger portion of the basilar membrane moves). This parallel input considerably reduces the time needed to perceive the tone (see [38], this volume).

Furthermore, it is more difficult to discern auditory signals when they are presented only for a short time, because the information is less regular for short signals. This fact is in accordance with experimental results (e.g. [34]). For a modeling study on the effects of stimulus duration on the hearing threshold see [16,40].

Ivey et al. [25] published their results on noise-induced tuning curve changes in mechano-receptors of the rat foot. They mechanically stimulated the mechano-receptors with waveforms comprised of various frequency sinusoidal waves in addition to increasing levels of white noise, and recorded spike activity of fibers from the tibial nerve using monopolar hook electrodes. The addition of noise enhanced signal transmission in the fibers: with increasing noise, the initially inverted V-shaped, zero-noise tuning curves broadened and eventually inverted. This effect can also be seen in our model for the mechano-receptor IHC (Fig. 8). The responses with added noise tended to be rate modulated at the low-frequency end, and followed nonlinear stochastic resonance (SR) properties at the higher frequencies.

Ivey et al. increased the noise and let the signal stay the same, whereas the modeling study presented here keeps the noise as it is determined by the biophysical reality (endogenous noise in the hair cell, Brownian motion of the stereocilia) and increases the snr by increasing the signal strength. These two ways of investigating the system are equivalent within the ranges investigated.

Close-to-threshold auditory signals in the low- or mid-frequency region are coded very efficiently. The spike train provides more information with roughly the same number of spikes as in the no stimulus case, where the spike train contains no information (spontaneous spiking). These high information rates come close to the fundamental physical limits of information transmission [42].

Especially in the highly sensitive mid-frequency regime, tones which cause displacements less than the thermal motions of the stereocilia are sufficient to cause sensation. The Brownian motion in this case enhances the ability to detect weak signals via the mechanism of SR (see also [16,48]).

This study showed that a compound model for the Brownian motion of IHC stereocilia, the mechano-electrical transduction including transduction channel gating noise, and the spike generation taking into account refractory period and jitter reproduces varying efficiency of the transmission of weak signals of several frequencies. Via the mechanism of SR, the Brownian motion of the stereocilia makes otherwise undetectable weak signals detectable. The jitter in the spiking times explains the steep slope in the threshold curve at higher frequencies (since phase-locking cannot be preserved). In the low-frequency regime, the short interspike times blunt the chance to detect the signal, but only for low snr.

The high-frequency results of this study give an answer to Gulick and co-workers [20] puzzle (italicized in the quote):

> "In summary, the form of the threshold curve is mainly a function of the transmission properties of the outer and middle ears. After these transmission properties have been taken into account, a relatively small effect of stimulus frequency on the psychophysical threshold remains. This residual effect must occur somewhere in the auditory system beyond the middle ear. According to Zwislocki, the locus of this residual effect is not to be found in the mechanical properties of the cochlea but, instead, in neurons of the central auditory system capable of temporal summation. However, *while this kind of analysis can account for the improved sensitivity from the low to the middle frequencies, it cannot account for the progressive loss of sensitivity from the middle to the high frequencies*."

Changes in hair bundle morphology also change the thermal fluctuations of the stereocilia and thereby the spontaneous spiking pattern in the cochlea nerve fibers. In the mildest cases of acoustic trauma, morphological changes are found only in the rootlets of the stereocilia, which become less dense in electron micrographs [33]. In more severe cases, leading to permanent damage, the stereocilia kink or fracture at the rootlet, and the packed actin filaments which give the stereocilia their rigidity are depolymerized [31, 51]. Within the IHC tuft, the damage to the tall, outer row of stereocilia is often selective: the shorter rows could remain ultrastructurally normal even when the tall row is completely missing; the tip links remain intact on the shorter stereocilia, suggesting that such IHCs might indeed be able to continue transduction, but with reduced sensitivity. Cochlear nerve fibers from these IHCs have much lowered rates of spontaneous activity [32]. Liberman and Dodds [33] also showed that following acoustic overstimulation, tuning curves with elevation of 'tips' and 'tails' were associated with significant decreases in the mean spontaneous discharge rates whereas tuning curves with elevated tips but hypersensitive tails were associated with clear elevation of the mean spontaneous rates. Altered Brownian motion patterns of the stereocilia contribute in the model to changes in the spiking pattern. However, one should bear in mind that in hearing loss of cochlear origin also other noise-induced changes, like different steady state Ca^{2+} concentrations due to altered Ca^{2+} pump kinetics, contribute to the pathological spiking patterns.

Further studies should take into consideration the varying patterns of the Brownian motion of the stereocilia which change along the tonotopical axis and which might be tuned to the enhancement of frequencies according to the tonotopical position of the IHC, any adaptation process of the transduction channels kinetics and the SR phenomena recently demonstrated in the transduction channels themselves (see Jaramillo and Wiesenfeld [26, 27], this issue pp. 1869–1874) as well as in the calcium-activated potassium channels in the basolateral hair cell membrane (Jaramillo, personal communication). Potassium conductances in the basolateral cell body membrane of IHCs from the guinea pig cochlea show a non-linearity in the voltage–current relationships, which might also lead to SR phenomena [29].

A cascade of SR effects at different stages of the mechano-electric transduction process might act together to establish the outstanding sensitivity of the hair cell.

Acknowledgements

I thank Frank Rattay and Tony Wenzelhuemer for critically reading the manuscript, Alice Mladenka, Richardson Naves Leao, Juliana Pontes-Pinto, Frank Rattay and Wolfgang Andreas Svrcek-Seiler for participating in preliminary studies on the subject and Jonathan Ashmore, Fernán Jaramillo, Steve Greenberg and Ted Evans for discussions.

References

[1] Blauert J. Spatial hearing: The psychophysics of human sound localization. Cambridge, MA: MIT Press, 1997.
[2] Cody AR, Russell IJ. The responses of hair cells in the basal turn of the guinea-pig cochlea to tones. J Physiol (Lond.) 1987;383:551–69.
[3] Crawford AC, Fettiplace R. The mechanical properties of ciliary bundles of turtle cochlear hair cells. J Physiol (Lond.) 1985;364:359–79.
[4] Crawford AC, Evans MG, Fettiplace R. The actions of calcium on the mechanoelectrical transducer current of turtle hair cells. J Physiol (Lond.) 1991;434:369–98.
[5] DeFelice LJ. Introduction to membrane noise. New York: Plenum Press, 1981.
[6] Denk W, Webb WW. Thermal noise limited transduction observed in mechano-sensory receptors of the inner ear. Phys Rev Lett 1989a;63:207–10.
[7] Denk W, Webb WW. Simultaneous recording of fluctuations of hair-bundle deflection and intracellular voltage in saccular hair cells. In: Wilson JP, Kemp DT, editors. Cochlear Mechanisms, Structure, Function and Models. New York: Plenum Press, 1989b;125–33.
[8] Denk W, Webb WW. Optical measurement of picometer displacements of transparent microscopic objects. Appl Opt 1990;29:2382–91.
[9] Denk W, Webb WW. Forward and reverse transduction at the limit of sensitivity studied by correlating electrical and mechanical fluctuations in frog saccular hair cells. Hear Res 1992;60:89–102.
[10] Denk W, Webb WW, Hudspeth AJ. Mechanical properties of sensory hair bundles are reflected in their Brownian motion measured with a laser differential interferometer. Proc Natl Acad Sci USA 1989;16:5371–5.

[11] Derksen HE. Axon membrane voltage fluctuations. Act Physiol et Pharmacol Neerl (Amsterdam) 1965;13:373–466.
[12] Derksen HE, Verveen AA. Fluctuations of resting neural membrane potential. Science 1966;151:1388–9.
[13] Ehrenberger K, Felix D. Glutamate receptors in afferent cochlear neurotransmission in guinea pigs. Hear Res 1991;52:73–80.
[14] Felix D, Ehrenberger K. The efferent modulation of mammalian inner hair cell afferents. Hear Res 1992;64:1–5.
[15] Felix H, Gleeson MJ, Pollak A, Johnsson L. The cochlear neurons in humans. In: Iurano S, Veldman JE, editors. Progress in human auditory and vestibular histopathology. Amsterdam: Kugler Publications, 1997;73–9.
[16] Gebeshuber IC, Mladenka A, Rattay F, Svrcek-Seiler WA. Brownian motion and the ability to detect weak auditory signals. In: Barbi M, Chillemi S, editors. Chaos and noise in biology and medicine (series in biophysics and biocybernetics). Singapore: World Scientific, 1998 (in press).
[17] Gitter AH, Frömter E, Zenner HP. C-type potassium channels in the lateral cell membrane of guinea-pigs outer hair cells. Hear Res 1992;60:13–9.
[18] Gleich O, Narins PM. The phase response of primary auditory afferents in a songbird (Sturnus vulgaris L.). Hear Res 1988;32:81–91.
[19] Greenwood DD. A cochlear frequency-position function for several species-29 years later. J Acoust Soc Am 1990;87:2592–605.
[20] Gulick WL, Gescheider GA, Frisina RD. Hearing – physiological acoustics, neural coding, and psychoacoustics. Oxford, New York: Oxford University Press, 1989.
[21] Harrison JM, Howe ME. Anatomy of the afferent auditory nervous system of mammals. In: Keidel WD, Neff WD, editors. Handbook of sensory physiology, vol. 5/1. Berlin: Springer, 1974;283–336.
[22] Hind JE. Physiological correlates of auditory stimulus periodicity. Audiology 1972;11:42–57.
[23] Hudspeth AJ. How the ear's works work. Nature 1989;341:397–404.
[24] Hudspeth AJ, Roberts WM, Howard J. Gating compliance, a reduction in hair-bundle stiffness associated with the gating of transduction channels in hair cells from the bullfrog's sacculus. In: Wilson JP, Kemp DT, editors. Cochlear mechanisms, structure, function and models. New York: Plenum Press, 1989;117–123.
[25] Ivey C, Apkarian AV, Chialvo DR. Noise-induced tuning curve changes in mechanoreceptors. J Neurophysiol 1998;79:1879–90.
[26] Jaramillo F, Wiesenfeld K. Mechanoelectrical transduction assisted by Brownian motion: a role for noise in the auditory system. Nature Neurosci 1998;1:384–8.
[27] Javel E. Acoustic and electrical encoding of temporal information. In: Miller JM, Spelman FA, editors. Cochlear implants – models of the electrically stimulated ear. Verlag: Springer, New York 1990;247.
[28] Katz B. Nerve, muscle and synapse. New York: McGraw-Hill, 1966.
[29] Kros CJ, Crawford AC. Potassium currents in inner hair cells isolated from the guinea-pig cochlea. J Physiol (Lond.) 1990;421:263–91.
[30] Lass Y, Abeles M. Transmission of information by the axon. I. Noise and memory in the myelinated nerve fiber of the frog. Biol Cybern 1975;8:61–7.
[31] Liberman MC. Auditory-nerve response from cats raised in a low-noise chamber. J Acoust Soc Am 1978;63:442–55.
[32] Liberman MC, Dodds LW. Single-neuron labeling and chronic cochlear pathology. II. Stereocilia damage and alterations of spontaneous discharge rates. Hear Res 1984;16:43–53.
[33] Liberman MC, Dodds LW. Acute ultrastructural changes in acoustic trauma: serial-section reconstruction of stereocilia and cuticular plates. Hear Res 1987;26:45–64.
[34] Mark HE, Rattay F. Frequency discrimination of single-, double- and triple-cycle sinusoidal acoustic signals. J Acoust Soc Am 1990;88:560–3.
[35] Markin VS, Jaramillo F, Hudspeth AJ. The three-state model for transduction-channel gating in hair cells. Biophys J 1993;64(2):93.
[36] Narins PM, Lewis ER. The vertebrate ear as an exquisite seismic sensor. J Acoust Soc Am 1984;76:1384–7.
[37] Nobili R, Mammano F, Ashmore J. How well do we understand the cochlea? Trends Neurosci 1998;21:159–67.
[38] Petracchi D. What is the role of stochastic resonance? Chaos, Solitons & Fractals 2000;11(12):1827–1834.
[39] Rattay F, Gebeshuber IC, Gitter AH. The mammalian auditory haircell: a simple electric circuit model. J Acoust Soc Am 1998a;103:1558–65.
[40] Rattay F, Mladenka A, Pontes J. Classifying auditory nerve patterns with neural nets: a modeling study with low level signals. Simulation Practice and Theory 1998b;6:493–503.
[41] Relkin EM, Doucet JR. Recovery from prior stimulation. I: relationship to spontaneous firing rates of primary auditory neurons. Hear Res 1991;55:215–22.
[42] Rieke F, Warland D, De Ruyter Van Steveninck R, Bialek W. Spikes: exploring the neural code (computational neuroscience). Cambridge: MIT Press, 1997.
[43] Rose JE, Hind JE, Anderson DJ, Brugge JF. Some effects of stimulus intensity on response of auditory nerve fibers in the squirrel monkey. J Neurophysiol 1971;34:685–99.
[44] Rose JE, Brugge JF, Anderson DJ, Hind JE. Phase-locked response to low-frequency tones in single auditory nerve fibers of the squirrel monkey. J Neurophysiol 1967;30:769–93.
[45] Sellick PM, Patuzzi R, Johnstone BM. Measurement of basilar membrane motion in the guinea pig using the Mössbauer technique. J Acoust Soc Am 1982;72:131–41.
[46] Sigworth FJ. An example of analysis. In: Sakmann B, Neher E, editors. Single-channel recording. New York: Plenum Press, 1985;301–21.
[47] Spoendlin H, Schrott A. Analysis of the human auditory nerve. Hear Res 1989;43:25–38.

[48] Svrcek-Seiler WA, Gebeshuber IC, Rattay F, Biro T, Markum H. Micromechanical models for the Brownian motion of hair cell stereocilia. J Theor Biol 1998;193:623–30.
[49] Zenner HP. Physiologische und biochemische Grundlagen des normalen und gestörten Gehörs (in German). In: Helms J, editor. Oto-Rhino-Laryngologie in Klinik und Praxis, vol. 1. Stuttgart: Ohr Georg Thieme Verlag, 1994;81–230.
[50] Zwicker E. Psychoakustik (in German). Berlin: Springer, 1982;34.
[51] Tilney LG, Saunders JC, Egelman E, DeRosier DJ. Changes in the organization of actin filaments in the stereocilia of noise-damaged lizard cochleae. Hear Res 1982;7:181–97.